

Two-Loop Analysis of the Pion Mass Dependence of the  $\rho$  MesonMalwin Niehus<sup>1,\*</sup>, Martin Hoferichter<sup>2,3,†</sup>, Bastian Kubis<sup>1,‡</sup> and Jacobo Ruiz de Elvira<sup>2,§</sup><sup>1</sup>Helmholtz-Institut für Strahlen- und Kernphysik (Theorie) and Bethe Center for Theoretical Physics, Universität Bonn, 53115 Bonn, Germany<sup>2</sup>Albert Einstein Center for Fundamental Physics, Institute for Theoretical Physics, University of Bern, Sidlerstrasse 5, 3012 Bern, Switzerland<sup>3</sup>Institute for Nuclear Theory, University of Washington, Seattle, Washington 98195-1550, USA

(Received 11 September 2020; accepted 2 February 2021; published 12 March 2021)

Analyzing the pion mass dependence of  $\pi\pi$  scattering phase shifts beyond the low-energy region requires the unitarization of the amplitudes from chiral perturbation theory. In the two-flavor theory, unitarization via the inverse-amplitude method (IAM) can be justified from dispersion relations, which is therefore expected to provide reliable predictions for the pion mass dependence of results from lattice QCD calculations. In this work, we provide compact analytic expression for the two-loop partial-wave amplitudes for  $J = 0, 1, 2$  required for the IAM at subleading order. To analyze the pion mass dependence of recent lattice QCD results for the  $P$  wave, we develop a fit strategy that for the first time allows us to perform stable two-loop IAM fits and assess the chiral convergence of the IAM approach. While the comparison of subsequent orders suggests a breakdown scale not much below the  $\rho$  mass, a detailed understanding of the systematic uncertainties of lattice QCD data is critical to obtain acceptable fits, especially at larger pion masses.

DOI: 10.1103/PhysRevLett.126.102002

*Introduction.*—While recent years have shown significant progress in understanding the QCD resonance spectrum from first principles in lattice QCD [1], most calculations are still performed at unphysically large pion masses, requiring an extrapolation to the physical point to make connection with experiment. Such extrapolations can be controlled using effective field theories, i.e., chiral perturbation theory (ChPT) [2–4] for observables that allow for a perturbative expansion. By definition, this precludes a direct application to resonances such as the  $\rho$  meson in the  $P$  wave of  $\pi\pi$  scattering. In fact, spectroscopy results from lattice QCD are arguably most advanced for the  $\rho$  meson [5–20], with even calculations at the physical point now available [20], which makes this channel the ideal example to study the details of the pion mass dependence. In addition, the  $\pi\pi$   $P$  wave features prominently in a host of phenomenological applications, among them hadronic vacuum polarization [21–26], nucleon form factors [27–30], and the radiative process  $\gamma\pi \rightarrow \pi\pi$  [31,32]. For the latter, a thorough understanding of the  $\pi\pi$   $P$  wave is prerequisite for an analysis of the pion mass dependence of recent lattice results [33–35],

see Ref. [36], and similarly for decays into three-pion final states [37].

On the technical level, the failure to produce resonant states is related to the fact that unitarity is only restored perturbatively in ChPT, so that any description of resonances requires a unitarization procedure. A widely used approach known as the inverse-amplitude method (IAM) achieves this unitarization by studying the unitarity relation for the inverse amplitude [38–46]. In particular, in the case of SU(2) ChPT the IAM procedure can be derived starting from a dispersion relation in which the discontinuity of the left-hand cut is approximated by its chiral expansion [41,42]. While Adler zeros induce a modification for the  $S$  waves [47], the naive derivation of the IAM survives for the  $P$ -wave amplitude: writing the partial wave for  $\pi\pi$  scattering  $t(s)$  as

$$t(s) = t_2(s) + t_4(s) + t_6(s), \quad (1)$$

with the subscripts indicating the chiral order, the unitarized amplitude at next-to-leading order (NLO) becomes [39–41]

$$t_{\text{NLO}}(s) = \frac{[t_2(s)]^2}{t_2(s) - t_4(s)}, \quad (2)$$

while at next-to-next-to-leading order (NNLO) [42,45]

Published by the American Physical Society under the terms of the Creative Commons Attribution 4.0 International license. Further distribution of this work must maintain attribution to the author(s) and the published article's title, journal citation, and DOI. Funded by SCOAP<sup>3</sup>.

$$t_{\text{NNLO}}(s) = \frac{[t_2(s)]^2}{t_2(s) - t_4(s) + [t_4(s)]^2/t_2(s) - t_6(s)}. \quad (3)$$

To assess the chiral expansion of the unitarized amplitude beyond the first term, one thus needs the partial-wave amplitudes at two-loop order [48].

The IAM has been applied to study resonance properties at unphysical pion masses at one- and two-loop order as early as in Refs. [49–52], with numerous subsequent works confronting the IAM predictions with lattice data [53–57]. However, apart from Refs. [51,52] such studies have been restricted to one-loop order, so that it was not possible to scrutinize the convergence properties of the expansion in the pion mass.

The reason for this situation was twofold. First, while the one-loop amplitudes can be given in analytic form, similarly compact expressions were not available for the two-loop amplitudes, thus complicating their implementation considerably. Second, as shown in Refs. [51,52], the increased number of low-energy constants (LECs) renders the fits more volatile, so that lattice data need to reach a sufficient quality to allow for meaningful two-loop fits. In this Letter we address both points: we present compact analytic expressions for the two-loop amplitudes that are straightforward to implement and devise a strategy for stable two-loop fits to current lattice data. While expressions are provided for all partial waves up to  $J = 2$ , we concentrate on the application to the  $\pi\pi P$  wave, including the resonance parameters of the  $\rho$  meson and its pole residue.

*Partial waves in ChPT.*—We express the partial waves  $t_J^I(s)$ , where  $I$  and  $J$  stand for the isospin and angular momentum, respectively, in terms of the pion decay constant in the chiral limit  $F$  as well as the pion mass  $M_\pi$  (including quark mass corrections from the LEC  $l_3^r$ ), to render the dependence on the physical pion mass explicit and exclude a spurious mass dependence arising from the transition  $F \rightarrow F_\pi$  [58]. We will follow the conventions of Refs. [3,61] for the one-loop LECs  $l_i^r$  and the two-loop LECs  $r_i^r$ . First, the leading-order (LO) results are [62]

$$\begin{aligned} t_0^0(s)|_2 &= \frac{2s - M_\pi^2}{32\pi F^2}, & t_0^2(s)|_2 &= -\frac{s - 2M_\pi^2}{32\pi F^2}, \\ t_1^1(s)|_2 &= \frac{s - 4M_\pi^2}{96\pi F^2}, & t_2^I(s)|_2 &= 0. \end{aligned} \quad (4)$$

At NLO, the partial-wave amplitudes can be written in the form [58]

$$\text{Re } t_J^I(s)|_4 = \sum_{i=0}^2 b_i^{IJ}(s)[L(s)]^i + \sum_{i=1}^3 b_i^{IJ}(s)l_i^r, \quad (5)$$

in terms of

$$L(s) = \log \frac{1 + \sigma(s)}{1 - \sigma(s)}, \quad \sigma(s) = \sqrt{1 - \frac{4M_\pi^2}{s}}, \quad (6)$$

and coefficient functions  $b_i^{IJ}(s)$ ,  $b_i^{IJ}(s)$ , which apart from phase-space and angular-momentum factors are polynomials in  $s$ . We find that the NNLO expressions can be brought into a very similar form,

$$\begin{aligned} \text{Re } t_J^I(s)|_6 &= \sum_{i=0}^4 c_i^{IJ}(s)[L(s)]^i + \sum_{i=1}^3 c_i^{IJ}(s)l_i^r \\ &+ d^{II}(s) \left\{ \sum_{n=\pm} \text{Li}_3[\sigma_n(s)] - L(s)\text{Li}_2[\sigma_-(s)] \right\} \\ &+ c_{l_3^r}^{IJ}(s)(l_3^r)^2 + P^{IJ}(s), \end{aligned} \quad (7)$$

where  $\sigma_\pm(s) = 2\sigma(s)/[\sigma(s) \pm 1]$ , and in addition to powers of  $L(s)$ , also polylogarithms  $\text{Li}_n$  appear. The contributions from the NNLO LECs are collected in  $P^{IJ}(s)$  and the imaginary parts determined by perturbative unitarity:

$$\text{Im } t_4(s) = \sigma(s)[t_2(s)]^2, \quad \text{Im } t_6(s) = 2\sigma(s)t_2(s)\text{Re } t_4(s). \quad (8)$$

*Fits to lattice data.*—From here on, we focus on the  $P$  wave of  $\pi\pi$  scattering, with both isospin  $I$  and angular momentum  $J$  equal to one. Its phase  $\delta(s) = \arg[t_1^1(s)]$  can be computed using lattice QCD via Lüscher's quantization condition [1,63], which allows one to determine the phase shift given  $\pi\pi$  energy levels and vice versa. To illustrate the fitting strategy as well as the conclusions regarding the pion mass dependence of  $\delta$  and the  $\rho$  parameters, we analyze such energy levels as computed on the lattice by two different groups. First, the one from Ref. [17], based on gauge configurations generated by the CLS collaboration, accompanied by a determination of the pion decay constant [64]. There are six datasets (ensembles) at five different pion masses in the range 200 to 284 MeV. Second, we consider the energy levels from the Hadron Spectrum Collaboration [12,65], using one of their ensembles with  $M_\pi \approx 236$  MeV and two with  $M_\pi \approx 391$  MeV. Both lattice calculations involve  $N_f = 2 + 1$  flavor simulations, but in either case the changes compared to the physical kaon mass, which determine the corrections to the LECs in two-flavor ChPT [66,67], are negligibly small compared to other sources of uncertainty. In the following, we concentrate mainly on the fit to the CLS data; details of the fitting procedure and the fits to the Hadron Spectrum data are given in Ref. [58]. To reduce the impact of scale-setting uncertainties, i.e., the error that arises when determining the lattice spacing in physical units, we work in lattice units wherever possible.

The fit proceeds as follows. At NLO, Eq. (2) is used to compute the phase  $\delta$ , which is subsequently inserted into

TABLE I. NLO LECs obtained from a fit to the CLS ensembles (evaluated at  $\mu = 0.77$  GeV). The first error is the statistical one, while the second arises due to the error of the lattice spacing. For comparison, in the second column the values expected from ChPT analyses are given, while the third column contains the values extracted from  $N_f = 2 + 1$  lattice QCD computations [72–77].

	Fit	Ref. [71]	Ref. [72]
$(l_2^r - 2l_1^r) \times 10^3$	12.62(25)(0)	9.9(1.3)	19(17)
$l_4^r \times 10^3$	-2.6(1.1)(0.2)	6.2(1.3)	3.8(2.8)

Lüscher’s quantization condition to determine the energy levels. Their distance to the energies as computed on the lattice is then minimized. Simultaneously, the pion decay constant is fit, using the ChPT expression truncated at NLO. In an NNLO fit, the same procedure is applied, with Eq. (3) instead of Eq. (2), and the pion decay constant truncated at NNLO. This means that at NLO only the LECs  $l_2^r - 2l_1^r$  and  $l_4^r$  appear, while the NNLO expressions depend on  $l_{1-4}^r$  as well as  $r_{a,b,c}$  and  $r_F^r$ .

The minimization of the  $\chi^2$  with respect to the fit parameters—most importantly the LECs—requires a sufficiently powerful algorithm. To find the global minimum, we first employ the differential evolution algorithm [68], whose results are subsequently refined via a modification of Powell’s method [69]. The former algorithm allows one to tackle the multidimensional, nonlinear optimization problem at hand in both a robust and efficient manner, if its parameters are adjusted carefully. Together with the improved lattice data the choice and tuning of this algorithm are crucial to obtain sound fits that are stable even when ensembles at only a few different pion masses are available, e.g., the two masses used by the Hadron Spectrum Collaboration.

There are three sources of error that need to be considered for a reliable uncertainty estimate: first, the statistical error of the lattice data; second, the error of the lattice spacing, which enters the ChPT expressions indirectly via the renormalization scale  $\mu$  [58]; third, the error that arises as a result of the truncation of the chiral expansion (1), which we are able to study in detail by a comparison of the IAM at one- and two-loop order. The chiral expansion proceeds in  $s/M_\rho^2$  as well as  $\alpha = M_\pi^2/M_\rho^2$ , with the breakdown scale expected to be set by the  $\rho$  mass since it is the lowest-lying resonance in the partial wave of interest. The energy dependence is resummed by the unitarization via the IAM, leaving the expansion in the pion mass as the most critical variable. Following Ref. [70], we estimate the truncation error of an observable  $X$  as

$$\Delta X_{\text{NLO}} = \alpha X_{\text{NLO}},$$

$$\Delta X_{\text{NNLO}} = \max \{ \alpha^2 X_{\text{NLO}}, \alpha |X_{\text{NLO}} - X_{\text{NNLO}}| \}. \quad (9)$$

*Results.*—To fix the LECs it is necessary to control both the  $s$  dependence and the mass dependence. Hence, we fit all

TABLE II. The same as Table I, but at NNLO. For the NNLO LECs we show the estimates from resonance saturation for comparison [78,79], although the uncertainties especially in  $r_{a,b}$  are substantial and difficult to quantify.

	Fit	Ref. [71]	Refs. [78,79]
$l_1^r \times 10^3$	-6.1(1.8)(0.1)	-4.03(63)	
$l_2^r \times 10^3$	2.58(90)(7)	1.87(21)	
$l_3^r \times 10^3$	0.776(65)(4)	0.8(3.8)	
$l_4^r \times 10^3$	-33(13)(0)	6.2(1.3)	
$r_a \times 10^6$	28(12)(1)		13
$r_b \times 10^6$	-4.8(2.6)(0.2)		-9.0
$r_c \times 10^6$	2.1(1.3)(0.1)		1.1
$r_F^r \times 10^3$	2.7(1.2)(0)		0

CLS ensembles from Ref. [17] simultaneously, once working to NLO and once working to NNLO, excluding only the ensemble N401 from the fit, since its pion decay constant has not been determined in Ref. [64]. To render the NNLO fit stable, it is necessary to put a constraint on the LEC  $l_3^r$ . This parameter governs the relation between the pion mass  $M_\pi$  and its value  $M$  at LO in ChPT, information on which is not included in our fit. Thus we add a penalty term to the  $\chi^2$  that favors values of  $l_3^r$  around its reference value  $0.8(3.8) \times 10^{-3}$  [71]. The LECs obtained at NLO are given in Table I, and the NNLO ones in Table II.

Since the amplitudes as given in Eqs. (2) and (3) have the appropriate analytic structure, they can be continued analytically to the second Riemann sheet, where the pole associated with the  $\rho$  resonance is located. Extracting the mass  $M_\rho$  and width  $\Gamma_\rho$  from the pole position  $s_p$  via  $s_p = (M_\rho - i\Gamma_\rho/2)^2$  and the coupling  $g$  of  $\rho$  to  $\pi\pi$  from the residue  $r$  via  $g^2 = 48\pi r / (4M_\pi^2 - s_p)$  yields the values shown in Table III. Also shown are the goodness of the fit as well as the obtained value of  $F$ , the pion decay constant in the chiral limit. The corresponding phase is depicted in Fig. 1. Here and in the following, the physical

TABLE III. Results of NLO and NNLO fits to the CLS data, including the goodness of the fit, the properties of the  $\rho$  resonance at the physical point, as well as the decay constant in the chiral limit. The first error is the statistical one, the second stems from the lattice spacing, the third is the truncation error estimated via Eq. (9). The Bayesian information criterion (BIC) is defined in terms of the number of fit parameters  $|\mathbb{F}|$  and the number of data points  $N$  as  $\text{BIC} = \chi^2 + |\mathbb{F}| \log N$ .

	NLO	NNLO
$\chi^2/\text{d.o.f.}$	216/(122 - 9) = 1.91	165/(123 - 15) = 1.53
BIC	259	237
$M_\rho/\text{MeV}$	761.4(5.1)(0.3)(24.7)	750(12)(1)(1)
$\Gamma_\rho/\text{MeV}$	150.9(4.4)(0.1)(4.9)	129(12)(1)(1)
$\text{Re } g$	5.994(54)(0)(194)	5.71(23)(2)(1)
$-\text{Im } g$	0.731(21)(0)(24)	0.46(14)(2)(1)
$F/\text{MeV}$	88.27(0.23)(0.04)(2.86)	93.7(2.3)(0.1)(0.2)

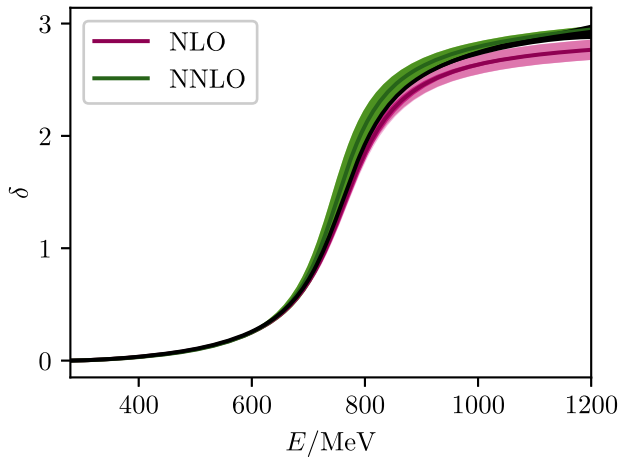


FIG. 1. The phase at physical pion mass as extrapolated from global fits to the CLS data; see Fig. 2 for color scheme. For comparison, in black the result of the dispersive analysis [22]. The extrapolation is performed at fixed  $E = \sqrt{s}$ , but a trajectory defined by fixed momentum instead would yield identical results.

point is simply defined by the Particle Data Group (PDG) value of the charged pion mass,  $M_\pi = 139.57$  MeV [80], and  $F$  is computed using the PDG value of  $F_\pi$  as input.

Because of the unitarization via the IAM, the LECs are expected to deviate to some extent from the ChPT reference values [41–44]. Accordingly, all LECs agree well with expectations, apart from a large discrepancy in  $l'_4$  both at NLO and NNLO. To understand its origin, we performed an NLO fit to the pion decay constant alone (at NNLO the fit becomes underconstrained), leading to  $l'_4 = 1.3(1.0) \times 10^{-3}$ , in agreement with the Flavour Lattice Averaging Group, but already in tension with phenomenology. The remainder of the pull displayed in Table I originates from the  $\pi\pi$  data. This pull becomes exacerbated at NNLO, but as indicated by the large uncertainties the sensitivity to  $l'_4$  is limited. Indeed, we observe only a moderate increase of the  $\chi^2$  if literature values of  $l'_4$  are enforced, as well as a large change to  $l'_4 = -16 \times 10^{-3}$  when employing a different strategy for the scale setting [17]. We conclude that there is

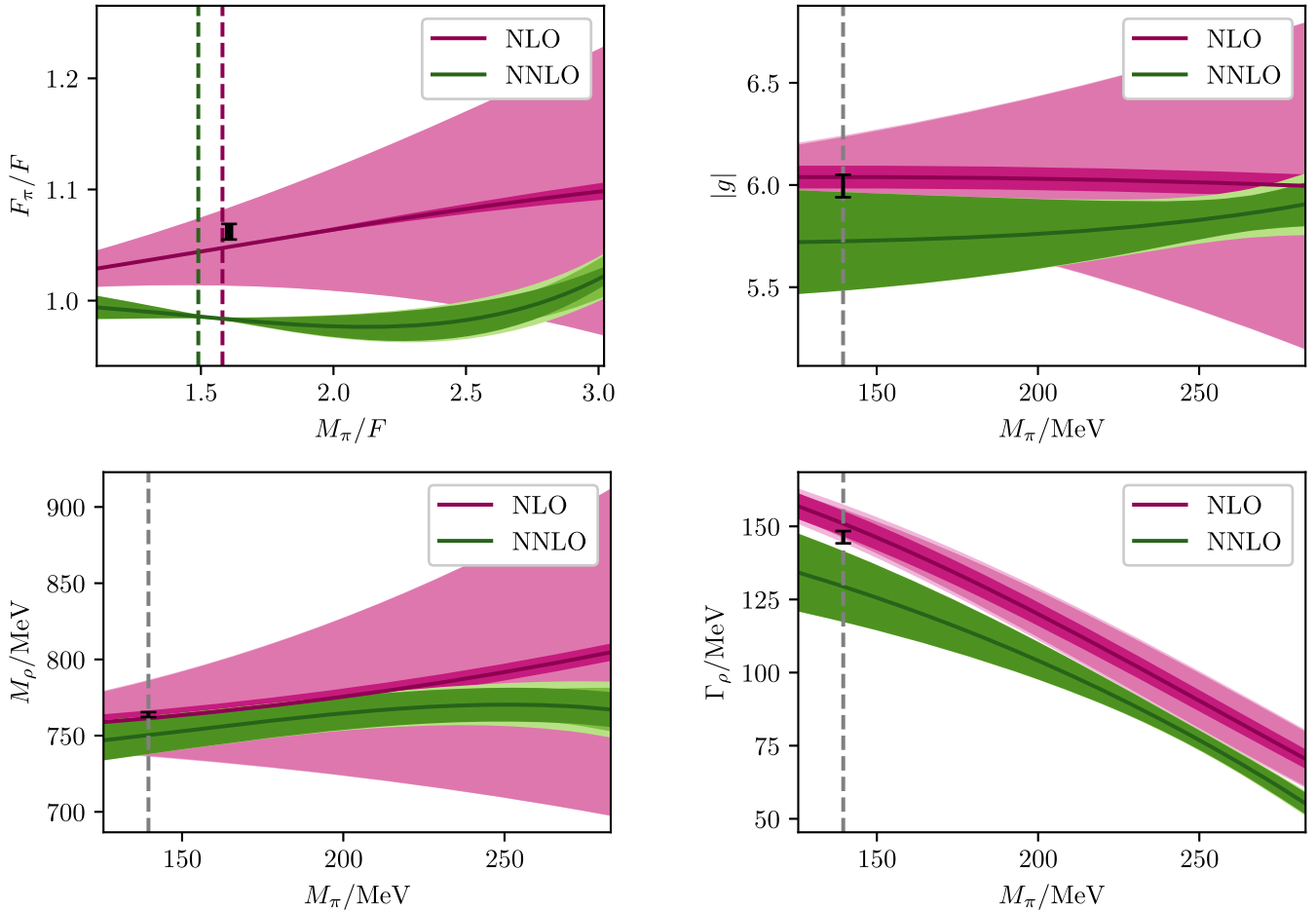


FIG. 2. The pion mass dependence of the decay constant, the coupling, as well as the real and imaginary part of the  $\rho$  pole as determined via fits to the CLS data, with error bands corresponding to (in order of decreasing color saturation) the data error (statistical plus spacing), the truncation error, and the total one. The dashed lines mark the physical pion mass. The decay constant is given in units of  $F$  to reduce the impact of the scale setting. Since the NLO and NNLO fits yield different values of  $F$ , their physical points in these units differ. Also shown as black ranges are reference values, the  $\rho$  characteristics taken from Ref. [82], and the decay constant from Refs. [72–77,80].

a tension between the pion decay constant in the chiral limit and  $\rho$  parameters, which at least in part may be related to scale-setting uncertainties [58].

In general, we note that the  $\chi^2/\text{d.o.f.}$  improves significantly when going from NLO to NNLO, although a statistically fully acceptable fit would require a more detailed understanding of lattice artifacts. Moreover, in the terms defined in Ref. [81],  $\Delta\text{BIC} = 22$  provides very strong evidence for the NNLO over the NLO IAM. Comparing the obtained  $\rho$  characteristics with the ones from Roy-like equations [82]—namely,  $M_\rho = 763.7^{+1.7}_{-1.5}$  MeV,  $\Gamma_\rho = 146.4^{+2.0}_{-2.2}$  MeV, and  $g = 5.98^{+0.04}_{-0.07} + i(-0.56)^{+0.10}_{-0.07}$ —shows that both the NLO and NNLO results are compatible with these already within statistical errors, with a  $1.4\sigma$  discrepancy in the width at NNLO and a  $2.2\sigma$  tension in  $\text{Im } g$  at NLO. However, only the NLO value of  $F$  is compatible with the literature value  $F = 86.89(58)$  MeV, which is obtained by combining the PDG value of  $F_\pi$  [80] with the Flavour Lattice Averaging Group  $N_f = 2 + 1$  average of  $F_\pi/F$  [72–77].

Our main results are shown in Figs. 1 and 2, for the pion mass dependence of the phase shift, the decay constant, and the  $\rho$  resonance parameters. Most notably, the two-loop analysis allows us to improve the precision considerably when going beyond the physical point, once the truncation becomes the dominant source of error. Second, with error bands produced assuming a breakdown scale of  $M_\rho$ , the NLO and NNLO bands mostly overlap, which indicates that the true breakdown scale of the theory may lie below the  $\rho$  mass, but not by much.

Overall, the coupling shows a very mild mass dependence [49,51], as does the  $\rho$  mass. Toward the end of the fit range, the central value of the two-loop curve seems to decrease, in disagreement with the phenomenological expectation from both the Kawarabayashi-Suzuki-Fayyazuddin-Riazuddin relation [83,84] and the expected ordinary  $q\bar{q}$  nature of the  $\rho$  meson [85]. This may again, in addition to the  $\chi^2$  and the tension in  $l'_4$ , point to the impact of lattice artifacts, which the two-loop IAM becomes flexible enough to mimic.

Similar conclusions can be drawn from the fits to the data by the Hadron Spectrum Collaboration [58]. They also show a significant improvement of the  $\chi^2$  when going from NLO to NNLO and a pion mass dependence that mimics the one depicted in Fig. 2, with the difference that  $M_\rho$  does not decrease at high pion masses, providing further evidence that this decrease may arise due to lattice artifacts. Notably, for the Hadron Spectrum data the  $\rho$  properties at the physical point are closer to the literature values at NLO than at NNLO.

*Conclusions.*—In this work we have presented compact analytic expressions for the two-loop partial-wave amplitudes for  $\pi\pi$  scattering up to  $D$  waves, with a first application to an analysis of lattice data for the  $P$ -wave amplitude and the  $\rho$  parameters. We have shown that two-loop fits do improve the fit quality and, by comparing NLO and NNLO results, found that the breakdown scale of the

chiral expansion should not lie much below the expected scale set by the  $\rho$  mass. However, we also concluded that the current datasets cannot be described in a statistically satisfactory way, with a more detailed understanding of the lattice data required.

In the future, anticipated improvements in the precision of lattice QCD calculations will increase the need to match that precision in the analysis. In this work, we have demonstrated how to achieve two-loop precision in practice, using the example of the  $P$  wave, but once lattice calculations mature a similar analysis can be performed for other partial waves including the pion mass dependence of the  $f_0(500)$ . Even once datasets at the physical point become available, the IAM will thus provide a tool for a high-precision analysis of lattice data.

Finite-volume energy levels taken from Refs. [12,65] were provided by the Hadron Spectrum Collaboration—no endorsement on their part of the analysis presented in the current paper should be assumed. In addition, we would like to thank John Bulava as well as ETMC for sharing lattice data with us. We thank Carsten Urbach for many useful discussions, and Raúl Briceño, Mattia Bruno, Christopher Thomas, Martin Ueding, Markus Werner, and David Wilson for valuable input. Financial support by the Bonn–Cologne Graduate School of Physics and Astronomy (BCGS), the DFG (CRC 110, “Symmetries and the Emergence of Structure in QCD”), the Swiss National Science Foundation, under Projects No. PCEFP2\_181117 (M.H.) and No. PZ00P2\_174228 (J.R.d.E.), and the DOE (Grant No. DE-FG02-00ER41132) is gratefully acknowledged.

\*niehus@hiskp.uni-bonn.de

†hoferichter@itp.unibe.ch

‡kubis@hiskp.uni-bonn.de

§elvira@itp.unibe.ch

- [1] R. A. Briceño, J. J. Dudek, and R. D. Young, *Rev. Mod. Phys.* **90**, 025001 (2018).
- [2] S. Weinberg, *Physica (Amsterdam)* **96A**, 327 (1979).
- [3] J. Gasser and H. Leutwyler, *Ann. Phys. (N.Y.)* **158**, 142 (1984).
- [4] J. Gasser and H. Leutwyler, *Nucl. Phys.* **B250**, 465 (1985).
- [5] S. Aoki *et al.* (CP-PACS Collaboration), *Phys. Rev. D* **76**, 094506 (2007).
- [6] M. Göckeler, R. Horsley, Y. Nakamura, D. Pleiter, P. Rakow, G. Schierholz, and J. Zanotti (QCDSF Collaboration), *Proc. Sci. LATTICE2008* (**2008**) 136 [arXiv:0810.5337].
- [7] X. Feng, K. Jansen, and D. B. Renner, *Phys. Rev. D* **83**, 094505 (2011).
- [8] C. B. Lang, D. Mohler, S. Prelovsek, and M. Vidmar, *Phys. Rev. D* **84**, 054503 (2011); **89**, 059903(E) (2014).
- [9] C. Pelissier and A. Alexandru, *Phys. Rev. D* **87**, 014503 (2013).
- [10] T. Metivet (Budapest-Marseille-Wuppertal Collaboration), *Proc. Sci. LATTICE2014* (**2015**) 079 [arXiv:1410.8447].

- [11] X. Feng, S. Aoki, S. Hashimoto, and T. Kaneko, *Phys. Rev. D* **91**, 054504 (2015).
- [12] D. J. Wilson, R. A. Briceño, J. J. Dudek, R. G. Edwards, and C. E. Thomas (Hadron Spectrum Collaboration), *Phys. Rev. D* **92**, 094502 (2015).
- [13] G. S. Bali, S. Collins, A. Cox, G. Donald, M. Göckeler, C. B. Lang, and A. Schäfer (RQCD Collaboration), *Phys. Rev. D* **93**, 054509 (2016).
- [14] D. Guo, A. Alexandru, R. Molina, and M. Döring, *Phys. Rev. D* **94**, 034501 (2016).
- [15] Z. Fu and L. Wang, *Phys. Rev. D* **94**, 034505 (2016).
- [16] C. Alexandrou, L. Leskovec, S. Meinel, J. Negele, S. Paul, M. Petschlies, A. Pochinsky, G. Rendon, and S. Syritsyn, *Phys. Rev. D* **96**, 034525 (2017).
- [17] C. Andersen, J. Bulava, B. Hörz, and C. Morningstar, *Nucl. Phys. B* **939**, 145 (2019).
- [18] M. Werner *et al.* (Extended Twisted Mass Collaboration), *Eur. Phys. J. A* **56**, 61 (2020).
- [19] F. Erben, J. R. Green, D. Mohler, and H. Wittig, *Phys. Rev. D* **101**, 054504 (2020).
- [20] M. Fischer, B. Kostrzewa, M. Mai, M. Petschlies, F. Pittler, M. Ueding, C. Urbach, and M. Werner (ETM Collaboration), [arXiv:2006.13805](https://arxiv.org/abs/2006.13805).
- [21] T. Aoyama *et al.*, *Phys. Rep.* **887**, 1 (2020).
- [22] G. Colangelo, M. Hoferichter, and P. Stoffer, *J. High Energy Phys.* **02** (2019) 006.
- [23] B. Ananthanarayan, I. Caprini, and D. Das, *Phys. Rev. D* **98**, 114015 (2018).
- [24] M. Davier, A. Hoecker, B. Malaescu, and Z. Zhang, *Eur. Phys. J. C* **80**, 241 (2020); **80**, 410(E) (2020).
- [25] A. Keshavarzi, D. Nomura, and T. Teubner, *Phys. Rev. D* **101**, 014029 (2020).
- [26] G. Colangelo, M. Hoferichter, and P. Stoffer, *Phys. Lett. B* **814**, 136073 (2021).
- [27] M. A. Belushkin, H.-W. Hammer, and U.-G. Meißner, *Phys. Rev. C* **75**, 035202 (2007).
- [28] I. T. Lorenz, U.-G. Meißner, H.-W. Hammer, and Y. B. Dong, *Phys. Rev. D* **91**, 014023 (2015).
- [29] M. Hoferichter, B. Kubis, J. Ruiz de Elvira, H.-W. Hammer, and U.-G. Meißner, *Eur. Phys. J. A* **52**, 331 (2016).
- [30] M. Hoferichter, B. Kubis, J. Ruiz de Elvira, and P. Stoffer, *Phys. Rev. Lett.* **122**, 122001 (2019); **124**, 199901(E) (2020).
- [31] M. Hoferichter, B. Kubis, and D. Sakkas, *Phys. Rev. D* **86**, 116009 (2012).
- [32] M. Hoferichter, B. Kubis, and M. Zanke, *Phys. Rev. D* **96**, 114016 (2017).
- [33] R. A. Briceño, J. J. Dudek, R. G. Edwards, C. J. Shultz, C. E. Thomas, and D. J. Wilson, *Phys. Rev. Lett.* **115**, 242001 (2015).
- [34] R. A. Briceño, J. J. Dudek, R. G. Edwards, C. J. Shultz, C. E. Thomas, and D. J. Wilson, *Phys. Rev. D* **93**, 114508 (2016).
- [35] C. Alexandrou, L. Leskovec, S. Meinel, J. Negele, S. Paul, M. Petschlies, A. Pochinsky, G. Rendon, and S. Syritsyn, *Phys. Rev. D* **98**, 074502 (2018).
- [36] M. Niehus, M. Hoferichter, and B. Kubis, *Proc. Sci. CD2018* (2019) 076.
- [37] M. Dax, T. Isken, and B. Kubis, *Eur. Phys. J. C* **78**, 859 (2018).
- [38] T. N. Truong, *Phys. Rev. Lett.* **61**, 2526 (1988).
- [39] A. Dobado, M. J. Herrero, and T. N. Truong, *Phys. Lett. B* **235**, 134 (1990).
- [40] T. N. Truong, *Phys. Rev. Lett.* **67**, 2260 (1991).
- [41] A. Dobado and J. R. Peláez, *Phys. Rev. D* **47**, 4883 (1993).
- [42] A. Dobado and J. R. Peláez, *Phys. Rev. D* **56**, 3057 (1997).
- [43] F. Guerrero and J. A. Oller, *Nucl. Phys. B* **537**, 459 (1999); **602**, 641(E) (2001).
- [44] A. Gómez Nicola and J. R. Peláez, *Phys. Rev. D* **65**, 054009 (2002).
- [45] J. Nieves, M. Pavón Valderrama, and E. Ruiz Arriola, *Phys. Rev. D* **65**, 036002 (2002).
- [46] A. Dobado and J. R. Peláez, *Phys. Rev. D* **65**, 077502 (2002).
- [47] A. Gómez Nicola, J. R. Peláez, and G. Ríos, *Phys. Rev. D* **77**, 056006 (2008).
- [48] J. Bijnens, G. Colangelo, G. Ecker, J. Gasser, and M. E. Sainio, *Phys. Lett. B* **374**, 210 (1996).
- [49] C. Hanhart, J. R. Peláez, and G. Ríos, *Phys. Rev. Lett.* **100**, 152001 (2008).
- [50] J. Nebreda and J. R. Peláez, *Phys. Rev. D* **81**, 054035 (2010).
- [51] J. R. Peláez and G. Ríos, *Phys. Rev. D* **82**, 114002 (2010).
- [52] J. Nebreda, J. R. Peláez, and G. Ríos, *Phys. Rev. D* **83**, 094011 (2011).
- [53] D. R. Bolton, R. A. Briceño, and D. J. Wilson, *Phys. Lett. B* **757**, 50 (2016).
- [54] B. Hu, R. Molina, M. Döring, and A. Alexandru, *Phys. Rev. Lett.* **117**, 122001 (2016).
- [55] M. Döring, B. Hu, and M. Mai, *Phys. Lett. B* **782**, 785 (2018).
- [56] B. Hu, R. Molina, M. Döring, M. Mai, and A. Alexandru, *Phys. Rev. D* **96**, 034520 (2017).
- [57] R. Molina and J. Ruiz de Elvira, *J. High Energy Phys.* **11** (2020) 017.
- [58] See Supplemental Material at <http://link.aps.org/supplemental/10.1103/PhysRevLett.126.102002>, which includes Refs. [59,60], for the explicit NLO and NNLO expressions of the  $\pi\pi$  partial waves and the pion decay constant as well as the details of the lattice data, fit strategy, error computation, scale-setting uncertainties, and the fits to the Hadron Spectrum data. The ChPT expressions are also provided in the form of a Mathematica notebook.
- [59] P. Virtanen, R. Gommers, T. E. Oliphant *et al.*, *Nat. Methods* **17**, 261 (2020).
- [60] R. G. Edwards, J. J. Dudek, D. G. Richards, and S. J. Wallace, *Phys. Rev. D* **84**, 074508 (2011).
- [61] J. Bijnens, G. Colangelo, and G. Ecker, *Ann. Phys. (N.Y.)* **280**, 100 (2000).
- [62] S. Weinberg, *Phys. Rev. Lett.* **17**, 616 (1966).
- [63] M. Lüscher, *Nucl. Phys. B* **354**, 531 (1991).
- [64] M. Bruno, T. Korzec, and S. Schaefer, *Phys. Rev. D* **95**, 074504 (2017).
- [65] J. J. Dudek, R. G. Edwards, and C. E. Thomas (Hadron Spectrum Collaboration), *Phys. Rev. D* **87**, 034505 (2013); **90**, 099902(E) (2014).
- [66] J. Gasser, C. Haefeli, M. A. Ivanov, and M. Schmid, *Phys. Lett. B* **652**, 21 (2007).
- [67] J. Gasser, C. Haefeli, M. A. Ivanov, and M. Schmid, *Phys. Lett. B* **675**, 49 (2009).

- [68] R. Storn and K. Price, *J. Global Optim.* **11**, 341 (1997).
- [69] W. H. Press, S. A. Teukolsky, W. T. Vetterling, and B. P. Flannery, *Numerical Recipes: The Art of Scientific Computing*, 3rd ed. (Cambridge University Press, Cambridge, England, 2007).
- [70] E. Epelbaum, H. Krebs, and U.-G. Meißner, *Eur. Phys. J. A* **51**, 53 (2015).
- [71] J. Bijnens and G. Ecker, *Annu. Rev. Nucl. Part. Sci.* **64**, 149 (2014).
- [72] S. Aoki *et al.* (Flavour Lattice Averaging Group), *Eur. Phys. J. C* **80**, 113 (2020).
- [73] A. Bazavov *et al.* (MILC Collaboration), *Proc. Sci. LATTICE2010* (**2010**) 074 [arXiv:1012.0868].
- [74] S. R. Beane, W. Detmold, P. M. Junnarkar, T. C. Luu, K. Orginos, A. Parreño, M. J. Savage, A. Torok, and A. Walker-Loud, *Phys. Rev. D* **86**, 094509 (2012).
- [75] S. Borsányi, S. Dürr, Z. Fodor, S. Krieg, A. Schäfer, E. E. Scholz, and K. K. Szabó, *Phys. Rev. D* **88**, 014513 (2013).
- [76] S. Dürr *et al.* (Budapest-Marseille-Wuppertal Collaboration), *Phys. Rev. D* **90**, 114504 (2014).
- [77] P. Boyle *et al.*, *Phys. Rev. D* **93**, 054502 (2016).
- [78] J. Bijnens, G. Colangelo, G. Ecker, J. Gasser, and M. E. Sainio, *Nucl. Phys.* **B508**, 263 (1997); **B517**, 639(E) (1998).
- [79] J. Bijnens, G. Colangelo, and P. Talavera, *J. High Energy Phys.* **05** (1998) 014.
- [80] P. Zyla *et al.* (Particle Data Group), *Prog. Theor. Exp. Phys.* **2020**, 083C01 (2020).
- [81] R. E. Kass and A. E. Raftery, *J. Am. Stat. Assoc.* **90**, 773 (1995).
- [82] R. García-Martín, R. Kamiński, J. R. Peláez, and J. Ruiz de Elvira, *Phys. Rev. Lett.* **107**, 072001 (2011).
- [83] K. Kawarabayashi and M. Suzuki, *Phys. Rev. Lett.* **16**, 255 (1966).
- [84] Riazuddin and Fayyazuddin, *Phys. Rev.* **147**, 1071 (1966).
- [85] J. Ruiz de Elvira, U.-G. Meißner, A. Rusetsky, and G. Schierholz, *Eur. Phys. J. C* **77**, 659 (2017).